Supporting Information

Calculation of the scattering cross-section

Form factor

For specular data, we calculate the form factor $\tilde{\rho}(q_z) = \left|\int \rho(z) e^{iq_z z} dz\right|^2$ using the 1G-hybrid model:

$$\begin{aligned}\tilde{\rho}(q_z) &= \frac{2(\rho_{CH_2} - \rho_{H_2O})\sin(q_z z_h)\cos(q_z \sigma_h)}{q_z(1-(2/\pi q_z \sigma_h)^2)} \\ &+ 2\sqrt{2\pi}\rho_h \sigma_h cos(q_z z_h)\exp(-1/2 q_z^2 \sigma_h^2) \\ &+ 2\sqrt{2\pi}\rho_{CH_3}\sigma_{CH_3} cos(q_z z_{CH_3})\exp(-1/2 q_z^2 \sigma_{CH_3}^2).\end{aligned} \tag{1}$$

Note that σ_h and σ_{CH_3} lump contributions not only from r.m.s. thermal fluctuations but also from the width of the transition between two neighboring regions.

For diffuse scattering data, we use the Fourier expansion:

$$\tilde{\rho}(q_z) = \int_{D/2}^{D/2} [\rho(z) - \rho_w] e^{-iqz} dz = \sum_{h=-h_{\max}}^{h_{\max}} F_h \frac{\sin(qD/2 - \pi h)}{(qD/2 - \pi h)}. \tag{2}$$

Height-height correlation function

To calculate the height-height correlation function $\langle z(\mathbf{0}) z(\mathbf{r}_\parallel)\rangle$, we take the Fourier transform the Helfrich thermal fluctuation spectrum $\langle z(q_\parallel) z(q_\parallel)\rangle$ (see main text) and obtain:

$$\langle z(\mathbf{0}) z(\mathbf{r}_\parallel)\rangle = \frac{k_B T}{2\pi\sqrt{\Delta}} \times \left[K_0(q_1 r_\parallel) - K_0(q_2 r_\parallel)\right], \tag{3}$$

where $\Delta = \gamma^2 - 4U''\kappa$. K_0 is the modified Bessel function of the second kind of order 0. For real arguments,

$$K_0(x)_{x\to 0} \approx Log2 - \gamma_E \; Log(x) \tag{4}$$

where γ_E is the Euler constant and $\lim_{x\to\infty} K_0(x) = 0$.

If $\Delta > 0$, q_1 and q_2 are real:

$$\begin{aligned} q_1 &= \sqrt{\left(\gamma - \sqrt{\Delta}\right)/2\kappa} \\ q_2 &= \sqrt{\left(\gamma + \sqrt{\Delta}\right)/2\kappa}. \end{aligned} \tag{5}$$

If $\Delta < 0$, they become complex:

$$\begin{aligned} q_1 &= \sqrt{(\gamma - i\sqrt{-\Delta})/2\kappa} \\ q_2 &= \sqrt{(\gamma + i\sqrt{-\Delta})/2\kappa}. \end{aligned} \tag{6}$$

For $|z| < 2$, following Abramovitz and Stegun [1], we use:

$$K_0(z) = -\left[\log\left(\frac{z}{2}\right) + \gamma_E\right] I_0(z) + z_d + \frac{3}{8}z_d^2 + \frac{11}{216}z_d^3 + \frac{25}{6912}z_d^4 + ... \tag{7}$$

with $z_d = 1/4z^2$ and $I_0(z) = \sum_{k=0}^{\infty} z_d^k/(k!)^2$, where I_0 is the modified Bessel function of the first kind of order 0.

For $|z| > 2$, we use:

$$K_0(z) = \sqrt{\frac{\pi}{2z}}e^{-z}\left[1 - \frac{1}{8z} + \frac{9}{2}\frac{1}{(8z)^2} - \frac{75}{2}\frac{1}{(8z)^3} + \frac{600}{(8z)^4} + ...\right]. \tag{8}$$

To calculate the scattered intensity, we insert the correlation function (Eq. 3) together with the appropriate form factor (Eq. 2) into the scattering cross-section (Eq. 3, main text).

The sensitivity to the parameters of the model is illustrated in Fig. 1.

Scattering by the ripple phase

To test the effect of possible static height-fluctuations, we calculate the scattering by ripples schematized in the insert of Fig. (2). The Fourier expansion is:

$$z(x) = \sum_{p=1}^{\infty} a_{2p+1} \sin\left[\frac{2\pi(2p+1)x}{\Lambda}\right], \tag{9}$$

with:

$$a_{2p+1} = \frac{2\Lambda^2}{(2p+1)^2\pi^2\Lambda_1(\Lambda - \Lambda_1)} \sin\left[(2p+1)\pi\left(1 - \frac{\Lambda_1}{\Lambda}\right)\right]. \tag{10}$$

Here x is a one-dimensional coordinate, and we obtain the height-height correlation function as a two-dimensional average over randomly oriented domains (powder diffraction diagram):

$$\langle z(0)z(r_\parallel)\rangle = \frac{1}{2}\sum_{p=1}^{\infty} a_{2p+1}^2 J_0\left[\frac{2\pi(2p+1)r_\parallel}{\Lambda}\right], \tag{11}$$

where J_0 is the Bessel function of the first kind of order 0. Inserting this correlation function in eq. 3 of the main text, we can estimate the scattering by a ripple phase.

While we do not know of publications reporting ripple phase in pure di-C_{18}-PC (DSPC), we can take order-of-magnitudes on related systems: di-C_{14}-PC (DMPC [2]), di-C_{16}-PC (DPPC [3]) and DSPC-DMPC mixtures [4].

Typical values correspond to a wavelength Λ in the range of ($\sim 10^{-9}$–10^{-7} m) and an amplitude of the order of 0.5–10 nm. Fig. (2) demonstrates that, on such examples, in this wavelength range our experiment has a sensitive detection level as low as (0.1–0.2 nm) in amplitude. A smoother undulation shape, resulting in a higher and narrower peak in Fourier space, would have been even easier to detect. To summarize, unless it had a very small wavelength (of order of 10^{-9} m, or less) [5], a static undulation like a ripple phase would certainly have been detected.

References

[1] M. Abramovitz and I. Stegun. Dover, New York, 1965.

[2] J.T. Woodward and J.A. Zasadzinski. *Biophys. J.*, 72:964, 1997.

[3] Y. Fang and J. Yang. *J. Phys. Chem.*, 100:15614, 1996.

[4] C. Leidy, T. Kaasgaard, J. H. Crowe, O. Mouritsen, and K. Jø rgensen. *Biophys. J.*, 83:2625–2633, 2002.

[5] B.A. Cunningham, A.D. Brown, D. H. Wolfe, W.P. Williams, and A. Brain. *Phys. Rev. E*, 58:3662, 1998.

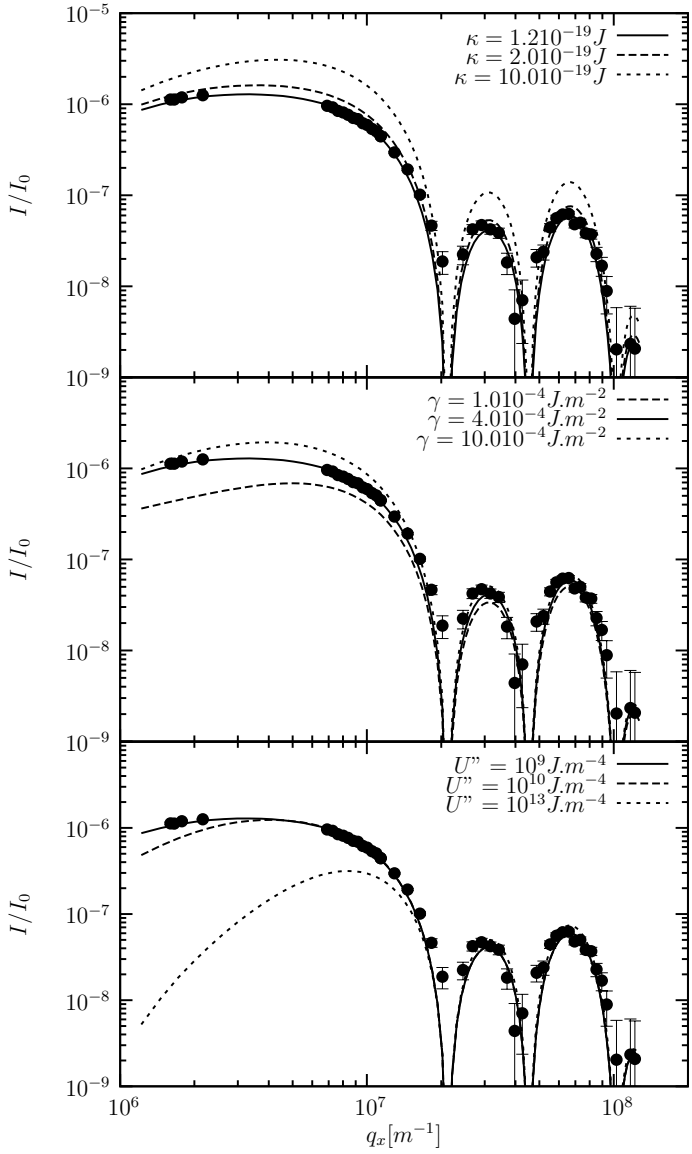

Figure 1: Sensitivity of the three-parameters fits. The solid line in each graph has been calculated using the values obtained by fitting the scattered intensity data for an adsorbed sample of di-C_{18}-PC at 51.5° (filled circles, shown for comparison): $U'' = 10^9\ Jm^{-4}$, $\gamma = 4 \times 10^{-4}\ Jm^{-2}$, $\kappa = 1.2 \times 10^{-19}\ J$ (see tables). Broken lines correspond to the modification of one parameter. Top: two experimentally-encountered values of $\kappa = 2 \times 10^{-19}\ J$ (long dashes), and $10 \times 10^{-19}\ J$ (short dashes). Middle: typical range of values for $\gamma = 10^{-4}\ Jm^{-2}$ (long dashes), and $10 \times 10^{-4}\ Jm^{-2}$ (short dashes). Bottom: $U'' = 10^{10}\ Jm^{-4}$ (long dashes) and $10^{13}\ Jm^{-4}$ (short dashes), corresponding to the extremes of the expected range of values.

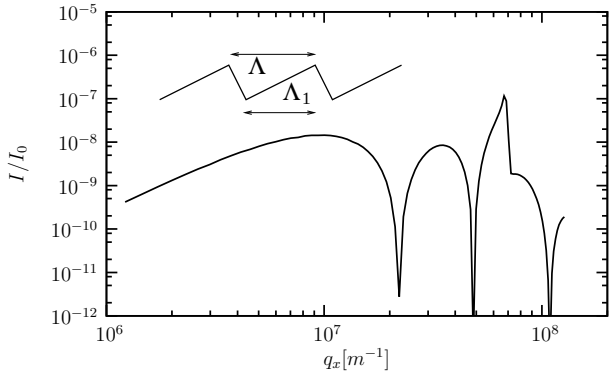

Figure 2: Ripple phase. The scattering curve is calculated for the ripple shape given in the insert with a peak-to-peak distance $\Lambda = 90\ nm$, a peak-to-well distance $\Lambda_1 = 40\ nm$ and a peak-to-well amplitude equal to $0.2\ nm$. Note the peak in the scattering reflecting the periodicity of the ripple.

Table 1: Structural parameters for di-C_{18}-PC, (adsorbed and grafted samples) at various temperatures: D: box thickness; ρ: electron density; σ: standard deviation of the box interface position (averaged over the coherence length $2\lambda/\theta\cdot\delta\theta$). Precisions are 10^{-1} nm, 10^{-2} nm, and 10^{-3} $e^-/\text{Å}^3$, respectively. Data are obtained by specular reflectivity experiments using the 1G-hybrid box model (eq. 1) in which some boxes lack D or σ. They are presented from top to bottom: bulk water 1, lipid layer 2 (floating bilayer), water layer 2 (intermediate), lipid layer 1 (adsorbed or grafted), water layer 1 (hydration), substrate. Abbreviations: h= head, sil=silane, Si=silicon.

		adsorbed sample		*grafted* sample
T	(°C)	25.0	56.1	57
ρ_{H_2O}	$(e^-/\text{Å}^3)$	0.344	0.344	0.344
$D_{h,2}$	(nm)	2.3	2.4	2.1
$\rho_{h,2}$	$(e^-/\text{Å}^3)$	0.116	0.136	0.120
$\sigma_{h,2}$	(nm)	0.60	0.30	0.35
ρ_{CH_2}	$(e^-/\text{Å}^3)$	0.320	0.269	0.320
ρ_{CH_3}	$(e^-/\text{Å}^3)$	-0.140	-0.145	-0.146
σ_{CH_3}	(nm)	0.17	0.15	0.15
ρ_{CH_2}	$(e^-/\text{Å}^3)$	0.320	0.269	0.320
$D_{h,2}$	(nm)	2.3	2.4	2.1
$\rho_{h,2}$	$(e^-/\text{Å}^3)$	0.116	0.136	0.120
$\sigma_{h,2}$	(nm)	0.60	0.30	0.35
$D_{H_2O,2}$	(nm)	1.9	2.4	2.2
$\rho_{H_2O,2}$	$(e^-/\text{Å}^3)$	0.344	0.344	0.344
$D_{h,1}$	(nm)	2.3	2.4	1.5
ρ_{h_1}	$(e^-/\text{Å}^3)$	0.114	0.120	0.120
$\sigma_{h,1}$	(nm)	0.39	0.41	0.35
ρ_{CH_2}	$(e^-/\text{Å}^3)$	0.290	0.269	0.320
ρ_{CH_3}	$(e^-/\text{Å}^3)$	-0.150	-0.145	-0.155
σ_{CH_3}	(nm)	0.14	0.30	0.36
ρ_{CH_2}	$(e^-/\text{Å}^3)$	0.290	0.269	0.320
$D_{h,1}$	(nm)	2.3	2.4	1.5
ρ_{h_1}	$(e^-/\text{Å}^3)$	0.114	0.120	0.120
$\sigma_{h,1}$	(nm)	0.39	0.41	0.35
$D_{H_2O,1}$	(nm)	0.3	0.3	
$\rho_{H_2O,1}$	$(e^-/\text{Å}^3)$	0.344	0.344	0.344
D_{sil}	(nm)			2.6
ρ_{sil}	$(e^-/\text{Å}^3)$			0.019
σ_{sil}	(nm)			0.25
D_{SiO_2}	(nm)	2.3	2.3	1.5
ρ_{SiO_2}	$(e^-/\text{Å}^3)$	0.338	0.338	0.269
σ_{SiO_2}	(nm)	0.13	0.27	0.25
ρ_{Si}	$(e^-/\text{Å}^3)$	0.376	0.376	0.376

Table 2: Parameters for di-C_{17}-PC grafted samples, obtained by off-specular experiments at various temperatures: Fourier coefficients (F_h) and pseudo-period D obtained from eq. (2); surface tension (γ) and bending modulus (κ). Error bars are incertitudes from the fits. $F_0 = 0$ for all samples.

T (°C)	F_1 ($e^-/\text{Å}^2$)	F_2 ($e^-/\text{Å}^2$)	F_3 ($e^-/\text{Å}^2$)	F_4 ($e^-/\text{Å}^2$)	D (nm)	γ ($10^{-4}\ Jm^{-2}$)	κ ($10^{-19}\ J$)
39	-1.8±0.15	-1.22±0.12	0.7±0.12	-1.22±0.12	6.5±0.25	5±3	10±4
44	-2.3±0.2	-1.3±0.2	0.9±0.15	-1.42±0.14	6.5±0.25	5±2.5	2±0.4
49	-2.3±0.1	-1.38±0.14	0.7±0.15	-1.39±0.12	6.4±0.25	4±0.5	1.6±0.5

Table 3: Parameters for di-C_{18}-PC grafted samples.

T (°C)	F_1 ($e^-/\text{Å}^2$)	F_2 ($e^-/\text{Å}^2$)	F_3 ($e^-/\text{Å}^2$)	F_4 ($e^-/\text{Å}^2$)	D (nm)	γ ($10^{-4}\ Jm^{-2}$)	κ ($10^{-19}\ J$)
48.0	-1.8±0.15	-1.1±0.15	0.6±0.2	-1±0.15	6.7±0.3	4±2	11±2
48.4	-1.5±0.15	-1.25±0.15	0.8±0.18	-1.1±0.15	6.9±0.3	5±1	10±3
51.1	-1.5±0.15	-1.1±0.15	0.7±0.18	-1.1±0.15	6.9±0.3	4±2.4	11±3
51.5	-2.4±0.2	-1.4±0.15	0.9±0.25	-1.6±0.2	6.75±0.25	4±1	1.2±0.4
52.8	-2.6±0.2	-1.0±0.1	0.9±0.3	-1.45±0.25	6.75±0.25	5±0.5	0.8±0.2
54.8	-2.5±0.2	-1.0±0.15	0.6±0.35	-1.5±0.2	6.45±0.25	3.5±1	2±0.6
56.1	-2.3±0.15	-1.1±0.15	0.8±0.3	-1.4±0.28	6.7±0.25	5±3	1.2±0.2
57.0	-2.4±0.3	-1.18±0.18	0.8±0.2	-1.3±0.3	6.7±0.27	5.5±1	0.8±0.04